Experimental Cell Research **258,** 109–120 (2000)
doi:10.1006/excr.2000.4907, available online at http://www.idealibrary.com on IDEAL®

Activation of Mitogen-Activated Protein Kinases Is Required for α_1-Adrenergic Agonist-Induced Cell Scattering in Transfected HepG2 Cells

Mark Spector,* Van-Anh Nguyen,* Xuening Sheng,* Liusheng He,† John Woodward,* Saijun Fan,‡ Clive M. Baumgarten,§ George Kunos,* Paul Dent,‖ and Bin Gao*,[1]

*Departments of *Pharmacology and Toxicology, §Physiology, and ‖Radiation Oncology, Medical College of Virginia of Virginia Commonwealth University, Richmond, Virginia 23298; †National Cancer Institute, National Institutes of Health, Bethesda, Maryland 20892; and ‡Department of Radiation Oncology, Long Island Jewish Medical Center, Albert Einstein College of Medicine, New York, New York 11040*

Activation of α_{1B}-adrenergic receptors (α_{1B}AR) by phenylephrine (PE) induces scattering of HepG2 cells stably transfected with the α_{1B}AR (TFG2 cells). Scattering was also observed after stimulation of TFG2 cells with phorbol myristate acetate (PMA) but not with hepatocyte growth factor/scatter factor, epidermal growth factor, or insulin. PMA but not phenylephrine rapidly activated PKCα in TFG2 cells, and the highly selective PKC inhibitor bisindolylmaleimide (GFX) completely abolished PMA-induced but not PE-induced scattering. PE rapidly activated p44/42 mitogen-activated protein kinase (MAPK), p38 MAPK, c-Jun N-terminal kinase (JNK), and AP1 (c-fos/c-jun). Selective blockade of p42/44 MAPK activity by PD98059 or by transfection of a MEK1 dominant negative adenovirus significantly inhibited the PE-induced scattering of TFG2 cells. Selective inhibition of p38 MAPK by SB203850 or SB202190 also blocked PE-induced scattering, whereas treatment of TFG2 cells with the PI3 kinase inhibitors LY294002 or wortmannin did not inhibit PE-induced scattering. Blocking JNK activation with a dominant negative mutant of JNK or blocking AP1 activation with a dominant negative mutant of c-jun (TAM67) significantly inhibited PE-induced cell scattering. These data indicate that PE-induced scattering of TFG2 cells is mediated by complex mechanisms, including activation of p42/44 MAPK, p38 MAPK, and JNK. Cell spreading has been reported to play important roles in wound repair, tumor invasion, and metastasis. Therefore, catecholamines acting via the α_1AR may modulate these physiological and pathological processes.

Key Words: **cell hypertrophy; protein kinase C; AP1.**

INTRODUCTION

α_1-Adrenergic receptors (α_1ARs)[2] are members of the G-protein-coupled receptor superfamily. Both pharmacological and molecular cloning studies have indicated the existence of multiple subtypes of α_1ARs including $\alpha_{1A/C}$AR, α_{1B}AR, and α_{1D}AR [1, 2]. α_1ARs play a key role in a variety of physiological processes, such as cardiac and smooth muscle contractility, contraction of the spleen, liver glycogenolysis, or melatonin secretion in the pineal gland [1, 2]. In addition to such short-term effects, α_1AR activation promotes cell proliferation and is also one of the most powerful hypertrophic signals in cardiac myocytes [3, 4]. This latter effect is reflected by significant changes in cell morphology, including increased cell size and cell volume and altered sarcomeric organization [3, 4]. Recent evidence implicates a variety of signaling pathways in α_1AR-induced cellular hypertrophy or hyperplasia. For example, activation of α_1AR stimulates liver regeneration and hepatocyte proliferation via p38 mitogen-activated protein kinase (p38 MAPK)- and c-Jun N-terminal kinase (JNK)-dependent pathways [5–9], whereas all three MAPKs, including p42/44 MAPK, p38 MAPK, and JNK, have been implicated in the cardiac hypertrophy induced by α_1AR agonists [10–16]. There is also evidence that activation of p70S6 kinase and PI3 kinase are involved in α_1AR-induced myocyte hypertrophy [17]. Both Rho and Ras are also involved in regulating myocardial cell growth and gene expression in response to α_1AR recep-

[1] To whom correspondence and reprint requests should be addressed at Department of Pharmacology and Toxicology, MCV/VCU, Box 980613, Richmond, VA 23298. Fax: (804) 828-2117. E-mail: BGAO@HSC.VCU.EDU.

[2] Abbreviations used: α_{1B}AR, α_{1B}-adrenergic receptor; TFG2 cells, HepG2 cells stably transfected with the α_{1B}-adrenergic receptor; PE, phenylephrine; HGF/SF, hepatocyte growth factor/scatter factor; EGF, epidermal growth factor; p42/44 MAPK, p42/44 mitogen-activated protein kinase; p38 MAPK, p38 mitogen-activated protein kinase; JNK, c-Jun N-terminal kinase; FAK, focal adhesion kinase; PMA, phorbol myristate acetate; PDBu, phorbol 12,13 dibutyrate; GFX, bisindolylmaleimide I (GF109203X); MBP, myelin basic protein; NP-40, Nonidet P-40; TCA, trichloroacetic acid.

0014-4827/00 $35.00

tor activation [14, 18, 19]. This is suggested by the finding that inhibition of Rho function by the dominant negative mutant N19RhoA or by *Clostridium botulinum* C3 transferase resulted in inhibition of PE-induced myocardial cell proliferation [18]. The role of Ras in cardiac hypertrophy is clearly demonstrated in Ras transgenic mice [19]. Activation of α_1AR also stimulates mitogenesis in human vascular smooth muscle cells and this effect is blocked by wortmannin [20]. This implicates PI3 kinase in α_1AR-mediated vascular smooth muscle cell proliferation. In rat isolated aortic smooth muscle cells that express α_{1D}AR and α_{1B}AR (but not α_{1A}AR), and in Rat-1 fibroblasts stably transfected with these three α_1AR subtypes, NE-induced cell growth is mediated by α_{1D}AR coupled to the MAPK pathway [21]. Activation of α_{1B}AR can also trigger uncontrolled cell growth during malignant transformation, as suggested by focus formation and disordered growth observed in Rat-1 fibroblasts transfected with the α_{1B}AR, or by the tumorigenic effect, reversible by prazosin, of transplanting such transfected cells into nude mice [22].

Although α_1AR agonists are powerful co-mitogens in the liver, the level of expression of α_{1B}AR is downregulated during hepatocyte proliferation [23]. For example, the tissue levels of α_{1B}AR and α_{1B}AR mRNA are high in the fully differentiated adult liver, whereas much lower levels are found in conditions associated with hepatocyte proliferation, such as primary culturing [24], partial hepatectomy [23, 25], fetal state [26], or malignant transformation [27, 28]. To understand the biological significance of such regulation, we generated a transfected HepG2 hepatoma cell line that stably expresses the α_{1B}AR at high levels (TFG2 cells). We have earlier reported that activation of α_{1B}AR in TFG2 cells inhibits cell growth via a p42 MAPK- and $p21^{Waf1/cip1}$-dependent mechanism [29]. In additional, unpublished studies we found that activation of α_{1B}AR in TFG2 cells by PE also induced cell scattering and hypertrophy which, to our knowledge, is a novel observation. Unexpectedly, these latter effects were independent of the activation of $p21^{Waf1/cip1}$. Therefore, in the present study we examined the signaling pathways involved in α_{1B}AR-induced cell scattering.

MATERIALS AND METHODS

Materials. P42/44 MAPK, p38 MAPK, JNK, and c-Jun antibodies (in solution and/or conjugated to protein A–agarose beads) were purchased from Santa Cruz Biotechnology (Santa Cruz, CA). Anti-phospho-p42/44 MAPK (Tyr^{204}) and anti-phospho-p38 MAPK (Thr^{180}/Tyr^{182}) antibodies were obtained from Bio-lab (Beverly, MA). Hormones, growth factors, myelin basic protein (MBP), phorbol 12-myristate 13-acetate (PMA), phorbol 12, 13 dibutyrate (PDBu), were obtained from Sigma Chemicals (St. Louis, MO). Pertussis toxin, PD98059, SB203850, SB202190, LY294002, wortmannin, and bisindolylmaleimide I (GF109203X) were from Calbiochem (San Diego, CA). Antibodies against PKC isoforms were purchased from GIBCO BRL (Grand Island, NY). Radiolabeled [γ-^{32}P]ATP was from Dupont, NEN (Boston, MA). Wild-type HepG2 human hepatocellular carcinoma cells were obtained from ATCC (Rockville, MD) and cultured under conditions specified by the supplier. The TFG2 cells were developed as reported earlier [29] and were cultured under the same conditions as the naive HepG2 cells, except for the additional presence of 0.5 mg/ml of geneticin to maintain selection pressure. The p69SV40T and M12 prostate cancer cells were kindly provided by Dr. Joy Ware [30]. The DU145 and PC3 prostate cancer cell lines were obtained from ATCC (Rockville, MD).

Cell scattering of TFG2 cells. HepG2 cells were stably transfected with rat α_{1B}AR cDNA to generate TFG2 cells, as described previously [29]. α_{1B}ARs in TFG2 cells were expressed at a density (1125 $\pm$ 30 fmol/mg of total cellular protein) similar to that in the normal adult rat liver (800 $\pm$ 30 fmol/mg membrane protein) [31].

About 2×10^3 TFG2 cells resuspended in culture medium were seeded on six-well plates (10 mm, Corning, NY). After 2 days, cells grown as discrete colonies were treated with various drugs for 30 min and then stimulated with 10^{-5} M phenylephrine (PE). After 16 h, the cells were washed with PBS to remove nonadherent cells, and then observed under a microscope and captured by a video camera. The pictures were saved as TIF files in Microsoft Powerpoint. For each condition, data were collected by random observation. Scattered cells were defined as cells with a flat and ameboid shape, lacking a round morphology, and not phase bright, whereas non-spread cells were rounded and grown as discrete colonies.

Western blot analysis. TFG2 cells were resuspended in 0.5 ml of homogeneization buffer A (20 mM Tris–HCl, 0.33 M sucrose, 2 mM EDTA, 0.5 mM EGTA, 2 mM PMSF, pH 7.5) and sonicated for 10 s, then spun at 100,000*g* for 1 h. The supernatant (cytosol fraction) was collected. The pellet (membrane fraction) was resuspended in 0.5 ml of buffer A with 1% NP-40, sonicated for 10 s, incubated on ice for 30 min, and spun at 100,000*g* for 30 min. The supernatant (membrane fraction) was then collected. Fifty micrograms of each sample was used in Western blotting. Western blot analysis, using streptavidine–alkaline phosphatase conjugated with nitroblue tetrazolium chloride and 5-bromo-4-chlor-3-indolphosphate *p*-toluidine salt as chromogens, was described previously [25].

[^{3}H]Thymidine incorporation. Following preincubation of TFG2 cells with an antagonist or vehicle for 24 h, [^{3}H]thymidine (2–5 μCi/ml) was added to the culture for 2 h. Cells were then dissolved by the addition of 1.0 ml of 0.5 N NaOH, collected, mixed with 1.5 ml of H_2O, and precipitated with 0.5 ml of 50% trichloroacetic acid (TCA). The precipitate was collected on glass filters, washed twice with 5% TCA, and the retained radioactivity determined by liquid scintillation spectrometry. Each time point for each set of experiment was determined in triplicate.

Measurement of cell size by flow cytometry. Control and PE-treated TFG2 cells were trypsinized, pelleted, washed once with Ca^{2+}- and Mg^{2+}-free PBS containing 1% BSA, and fixed in 70% ethanol. Prior to flow cytometry, the fixed cells were pelleted for 5 min at 1500 rpm and washed again with 1$\times$ PBS to remove residual ethanol, and then stained in 5 μg/ml PI in PBS with RNase at dark, for at least 20 min at 4°C. The samples were analyzed by FACS cytometry (BD). Small-angle forward scatter (FCS) was used as a measure of cell size. DNA content was measured as fluorescence of PI by FL2. Ten thousand cells were run for each sample.

Transient transfection of α_{1B}AR into prostate cancer M12 cell line. α_{1B}ARs in pcDNA3 expression vector were transfected into M12 cells by the adenovirus–lysine-mediated procedure as described previously [32, 33]. Adenovirus–DNA complexes were prepared by incubating lysine-modified adenovirus with α_{1B}AR expression vector for 30 min at 25°C in the dark, followed by a 30-min incubation with polylysine at a molar concentration equivalent to 125 times the molar plasmid DNA concentrations. The adenovirus–DNA–lysine complex in serum-free medium was added to the cells and incubated

for 8 h at 37°C. Serum was then added and the cells were cultured for a further 48–72 h.

Kinase assays for p42/44 MAPK, p38 MAPK, and JNK. TFG2 cells grown in 100-mm dishes were serum-starved overnight and then stimulated with various drugs for various time periods. The stimulated TFG2 cells were homogenized in 400 μl of ice-cold lysis buffer A (25 mM Hepes, pH 7.4, 5 mM EDTA, 5 mM benzamidine, 1 mM phenylmethyl sulfonylfluoride, 1 mg/ml soybean trypsin inhibitor, 40 μg/ml pepstatin A, 40 μg/ml aprotinin, 1 μM Microcystin-LR, 0.5 mM sodium orthovanadate, 0.5 mM sodium pyrophosphate, 1% (v/v) Triton X-100, 0.1% (v/v) 2-mercaptoethanol). The homogenate was incubated on ice for 5 min. After centrifugation at 14,000*g* for 10 min, the supernatant was collected and protein concentration was measured using the Bio-Rad protein assay reagent. The supernatant was subjected to kinase assays, as described below.

Protein A/G plus agarose slurry (25 μl bead volume) was washed with 1 ml PBS containing 0.1% (v/v) Tween 20 and resuspended in 0.4 ml of the same buffer. P42/44 MAPK, p38 MAPK, or JNK antibodies (2 μg in 20 μl) were added to each tube and incubated (2 h, 4°C) to allow for their conjugation to protein A/G plus agarose beads, followed by a subsequent wash to remove nonconjugated antibodies. Five hundred micrograms of protein from each homogenate was mixed with protein A agarose-conjugated antibody and rocked (2 h, 4°C). The protein A agarose was recovered by centrifugation, the supernatant was discarded, and the immunoprecipitates were washed twice with lysis buffer A and once with washing buffer B (25 mM Hepes, pH 7.4, 15 mM $MgCl_2$, 0.1 mM sodium orthovanadate, 0.1% (v/v) 2-mercaptoethanol).

The p42/44 MAPK and p38 MAPK assays have been described previously [8]. Briefly, immunoprecipitates were incubated (final volume 50 μl) with 50 μl of washing buffer B containing 0.2 mM [γ-^{32}P]ATP (5000 cpm/pmol), 1 μM Microcystin-LR, and 1 mg/ml MBP. In preliminary experiments, the kinase activities were linear with respect to incubation time between 2 and 40 min. Therefore, samples were incubated for 15 min, and then 40 μl of the reaction volume was spotted onto P81 paper (Whatman, Maidstone, UK) and immediately placed into 180 mM phosphoric acid. The papers were washed several times with phosphoric acid, followed by a final wash with acetone. The ^{32}P incorporation into MBP was quantified by liquid scintillation spectrometry. Alternatively, the reactions were terminated with SDS protein loading buffer and prepared for SDS–PAGE (15% polyacrylamide gel) to quantify ^{32}P incorporation by phosphorimaging.

The JNK activity was measured as described previously [8]. Briefly, immunoprecipitates were incubated (final volume 50 μl) with 50 μl of washing buffer B containing 0.2 mM [γ-^{32}P]ATP (5000 cpm/pmol), 1 μM Microcystin-LR, and 10 μg GST-c-Jun (amino acids 1–169). After 30 min, the reactions were terminated with SDS protein loading buffer and the mixtures prepared for SDS–PAGE (15% polyacrylamide gel) to quantify ^{32}P incorporation by phosphorimaging.

P42/44 MAPK and p38 MAPK activities were also detected in Western blotting analysis by using specific anti-phospho-p42/44 MAPK and anti-phospho-p38 MAPK, respectively.

Adenovirus infection of TFG2 cells. TFG2 cells were cultured in DMEM containing 10% fetal calf serum, washed with serum-free medium, and then infected with either null recombinant adenovirus or with dominant-negative MEK1−/−, JNK, or c-jun (TAM) recombinant adenovirus in a total volume of 0.5 ml and at a multiplicity of infection of 250. After infection for 8 h at 37°C, the cells were washed with serum-free medium and cultured for a further 24 h prior to stimulation with PE. The recombinant adenovirus dominant negative MEK1−/− and JNK were described previously [8, 9]. The recombinant adenovirus dominant-negative c-jun (TAM67) recombinant adenovirus was generated from wild-type c-Jun by deletion of residues 3–122 in the amino-terminal transcriptional activation domain [34].

Gel mobility shift assays. Gel mobility shift assays were described previously [35]. The AP1 oligo (5′-CGC TTG ATG AGT CAG CCG GAA -3′) was used as a probe.

RESULTS

Activation of α_{1B}AR by PE Induces Morphological Changes of TFG2 Cells, Including Scattering, Increased Cell Size, and Formation of Processes

In the unstimulated state, the morphology of TFG2 cells is similar to that of the mock-transfected or wild-type HepG2 cells. As shown in Fig. 1A, when these cells are plated sparsely, they proliferate as discrete colonies. After stimulation of TFG2 cells with PE for 8–12 h, the cells start to "scatter" and detach from each other, and by 16 h most cells become scattered. After 4 days, about 60% of the cells extend multiple cellular processes. A number of these processes reach several cell diameters in length, and all of them terminate in growth-cone-like structures. The scattered cells appear well-extended and elongated and have a "flattened" morphology. PE did not induce scattering of mock-transfected HepG2 cells, and the PE-induced scattering of TFG2 cells was completely prevented by 1 μM prazosin (data not shown), which indicates the involvement of α_1AR. The overall size of the cells appears increased after stimulation with PE, which is confirmed by flow cytometry. Control and PE-treated TFG2 cells were trypsinized, fixed with 70% ethanol, stained with PI, and analyzed by FACS cytometry using a small-angle forward scatter. As illustrated in Fig. 1B, PE treatment significantly increased cell size. All of the above effects of PE were observed in cells maintained in medium containing 10% serum. Similar effects were observed when TFG2 cells were maintained in serum-free medium (our unpublished data), which suggests that these effects are serum-independent.

We also tested whether other agonists have effects similar to those produced by PE in TFG2 cells. As shown in Fig. 1A, when the cells were treated with PMA or PDBu for 15 min and then washed free of the drug, they became completely spread out within 12 h following treatment. It has been reported that 10 ng/ml of HGF/SF rapidly and significantly induces scattering of MDCK epithelial cells [36]. However, treatment of HepG2 cells with 10 ng/ml of HGF/SF for 24 h did not induce cell scattering (Fig. 1A), and partial scattering could be seen only at a very high (500 ng/ml) concentration of HGF/SF (not shown). This suggests that HGF/SF does not induce scattering of HepG2 cells. Treatment of TFG2 cells with EGF, insulin, or NGF for 24 h did not cause cell scattering. Partial scattering was observed after incubation of TFG2 cells with EGF for several days (data not shown). The effect of these agonists on TFG2 cell proliferation was also studied. Treatment with PE and PMA caused 50 and 40% inhi-

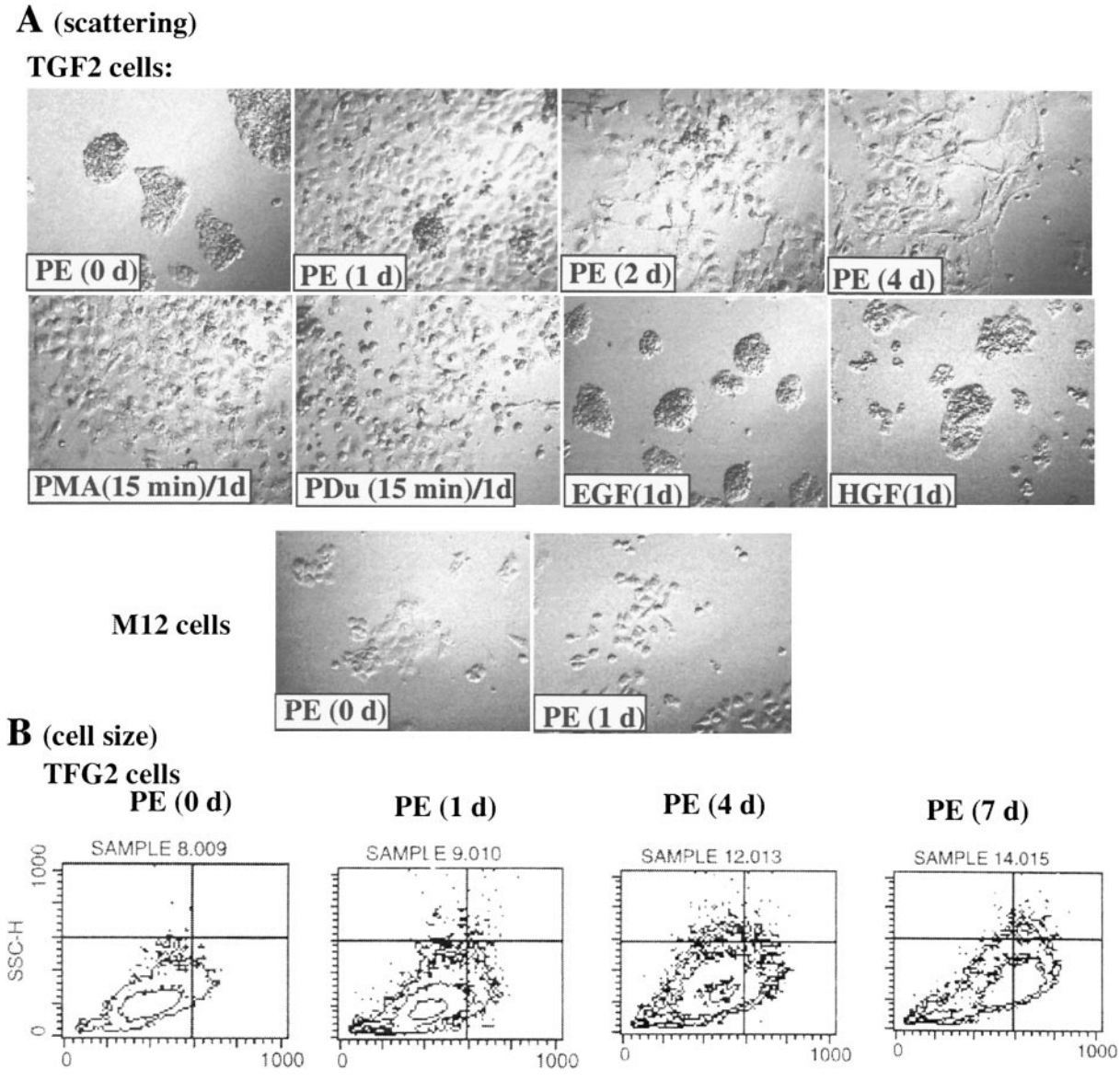

FIG. 1. Activation of α_{1B}AR by PE induces morphological changes of TFG2 cells, including scattering, increases in cell size, and formation of processes. (A) TFG2 cells or M12 prostate cancer cells were treated with 10^{-5} M PE for 1–4 days or with 10^{-5} M PMA or 10^{-5} M PDbu for 15 min and then transferred to fresh growth medium for 1 day, or treated with 10 ng/ml of EGF + 50 ng/ml of HGF for 1 day. The cells were then observed under a microscope and the images captured by a video camera. For each condition, data were collected by random observation. (B) TFG2 cells were treated with 10^{-5} M PE for 1–7 days and then subjected to FACS cytometry (BD) under small-angle forward scatter (FCS) for measurement of cell size, as described under Material and Methods.

bition of [^{3}H]thymidine uptake, respectively, while treatment with EGF, insulin, or NGF stimulated TFG2 cell proliferation. The PMA-induced inhibition of cell proliferation and scattering were also observed in mock-transfected HepG2 cells (data not shown). Although, as mentioned above, low concentrations of HGF did not induce TFG2 cells to scatter, HGF significantly inhibited [^{3}H]thymidine uptake in both HepG2 and TFG2 cells, which suggests that HGF receptor signaling is functional in these cells.

It has been reported that α_1ARs are expressed at high levels in human prostate cancer tissue [37]. We therefore tested whether activation of α_1AR also induces scattering of prostate cancer cells. Surprisingly, levels of α_1AR binding were undetectable or very low in four prostate cancer cell lines, including p69SV40T [30], M12 [30], DU145, and PC3 cells (unpublished data). Therefore, in order to examine the effect of PE on scattering of prostate cancer cells, we transfected α_{1B}AR into M12 cells by using the lysine–adenovirus procedure. By using this technique, transfection efficiencies of ~80% can be achieved [32]. As shown in Fig.

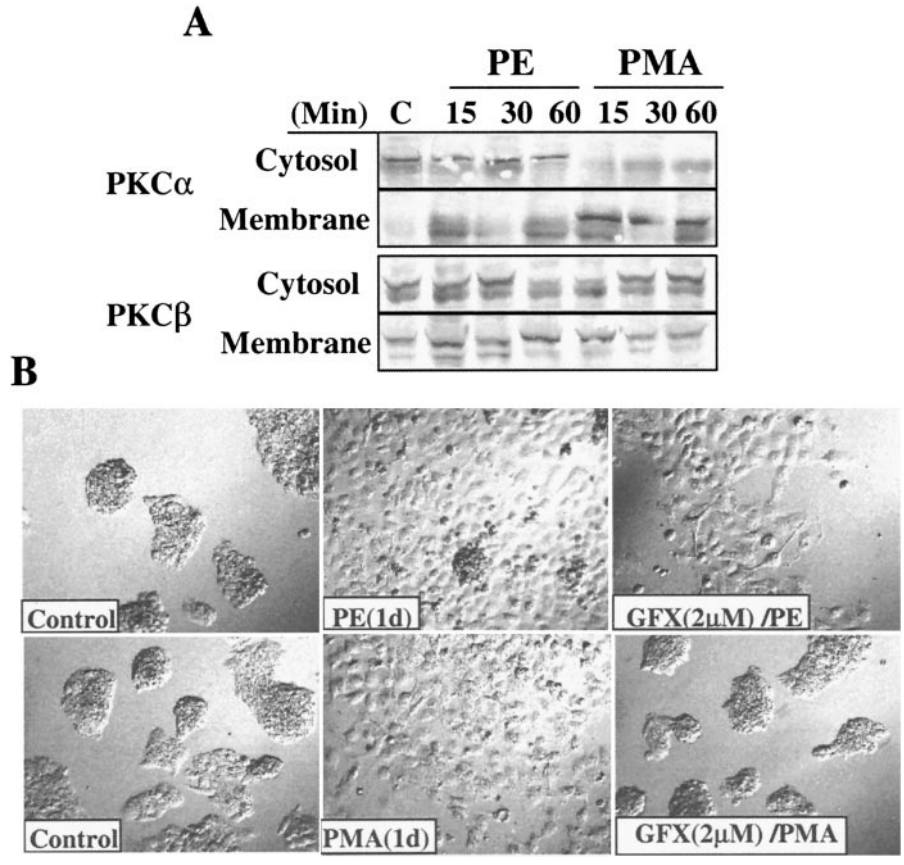

FIG. 2. PE-induced scattering of TFG2 cells is PKC-independent while PMA-induced scattering of TFG2 cells is PKC-dependent. (A) TFG2 cells were stimulated with 10^{-5} M PE or PMA for 15 to 60 min and then the cytosol and membrane proteins were isolated and analyzed by Western blotting using anti-PKC antibodies. (B) TFG2 cells were treated with GFX for 30 min and then stimulated with 10^{-5} M PE or PMA. After 16 h, the cells were observed under microscope and the pictures were captured by a video camera.

1A, PE treatment induced marked scattering of M12 cells transfected with α_{1B}AR but not in mock-transfected cells, which suggests that PE-induced cell scattering is not unique to HepG2 cells.

PE-Induced Scattering of TFG2 Cells Is PKC-Independent while PMA-Induced Scattering Is PKC-Dependent

It is well established that activation of PKC in various cell types is associated with its translocation from the cytosol to the membrane. To test whether PKC is activated during PE- or PMA-induced scattering of TFG2 cells, we analyzed immunoreactive PKCα and PKCβ in cytosolic and membrane fractions using Western blotting. As shown in Fig. 2A, exposure of TFG2 cells to PMA causes a complete translocation of PKCα from cytosol to membrane. Unexpectedly, PE did not elicit a significant translocation of PKCα in these cells (Fig. 2A). Both PMA and PE caused only a slight shift of PKCβ from cytosol to membrane. This suggests that PMA but not PE activates PKC in TFG2 cells. To examine directly whether PKC activation is involved in PE- or PMA-induced scattering of TFG2 cells, we tested the effects of a highly selective PKC inhibitor, GF109203X (GFX). As shown in Fig. 2B, GFX (0.2 μM) completely blocked the PMA-induced, but only slightly inhibited the PE-induced, scattering. The same concentration of GFX also completely blocked PMA-induced p42/44 MAPK activation (data not shown). These results suggest that the PE-induced scattering of TFG2 cells is PKC-independent whereas the PMA-induced scattering is PKC-dependent.

Activation of p42/44 MAPK and p38 MAPK but Not PI3 Kinase Is Required for the PE-Induced Scattering of TFG2 Cells

Activation of p42/44 MAPK plays an important role in cell proliferation and induces morphological changes including hypertrophy in myocytes [36, 38–40]. We tested whether this kinase is also involved in the α_1AR-induced scattering of TFG2 cells. As shown in Fig. 3A, PE rapidly activated p42/44 MAPK that peaked at 10

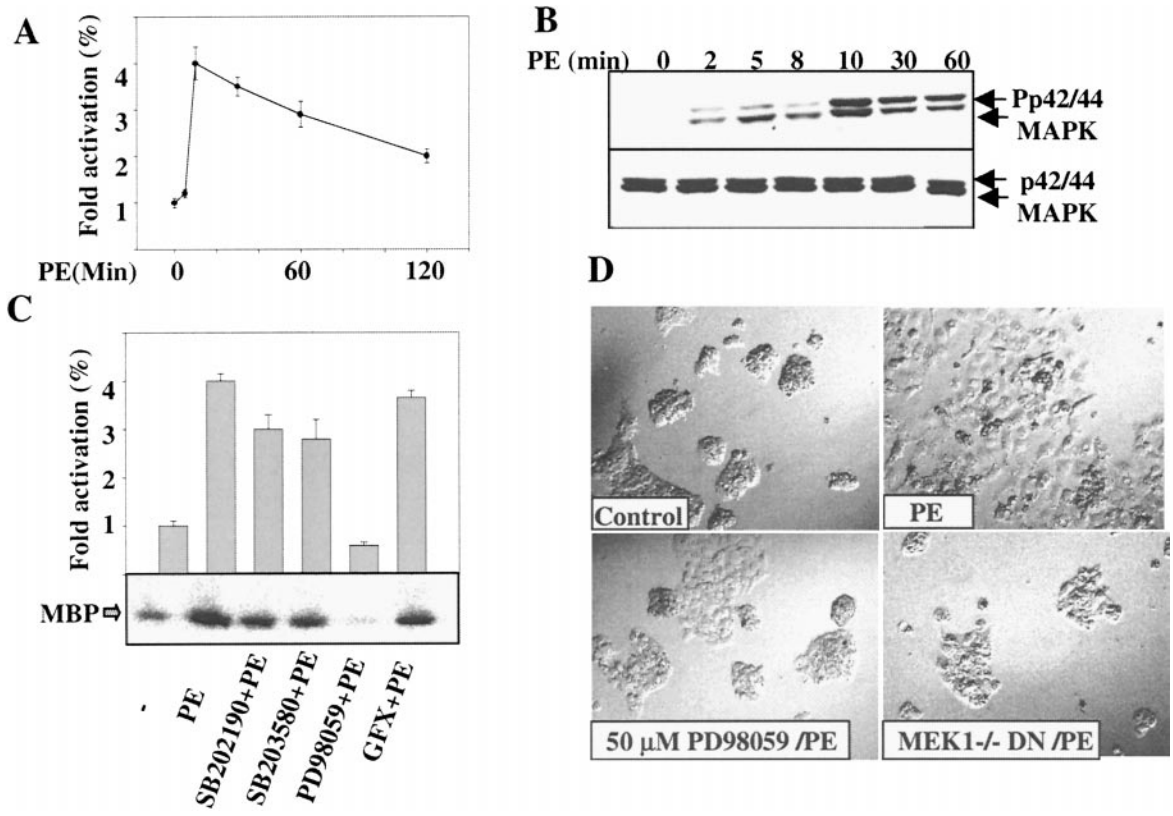

FIG. 3. PE-induced scattering of TFG2 cells is p42/44 MAPK-dependent. (A) and (B) TFG2 cells were stimulated with PE for various times and then cell lysates were prepared for either p42/44 MAPK assays by using MBP as a substrate (panel A) or Western blotting analysis by using a specific anti-phospho-p42/44 MAPK antibody (panel B). (C) TFG2 cells were treated with 5 μM SB203580, 5 μM SB202190, 50 μM PD 98058, or 2 μM GFX for 30 min as indicated, and then stimulated with 10^{-5} M PE for 10 min, after which cell lysates were prepared for p42/44 MAPK assay by using MBP as a substrate. In panels A, B, and C, autoradiograms representative of three independent experiments are shown. The radioactivities on blots from three independent experiments were quantified by phosphorimaging. Values shown are means ± SE from three independent experiments, expressed as fold changes over control. (D) TFG2 cells were treated with PD98059 for 30 min and then stimulated with 10^{-5} M PE for 16 h, or were infected with a recombinant adenovirus expressing a dominant-negative MEK1−/−. After 24 h, cells were incubated with 10^{-5} M PE for an additional 16 h. The cells were observed under a microscope and the pictures were captured by a video camera.

min, and activity remained elevated twofold for at least 2 h. PE activation of p42/44 MAPK was further confirmed by Western blotting analysis using a specific anti-phospho-p42/44 MAPK antibody (Fig. 3B). Pretreatment with the specific PKC inhibitor GFX did not inhibit PE-induced p42/44 MAPK activation (Fig. 3C) but completely abolished PMA-induced p42/44 MAPK activation (data not shown). This suggests that PE-induced p42/44 MAPK activation is PKC-independent, which is consistent with previous observations of PE-induced p42/44 MAPK activation in transfected HEK-293 cells by calcium-dependent and PKC-independent mechanisms [41]. We have previously shown that blocking p42/44 MAPK with the specific MEK1 inhibitor PD98059 or by transfection of a dominant-negative MEK1 recombinant adenovirus blunted the PE-induced inhibition of TFG2 cell proliferation [29]. The same treatments also significantly inhibited the PE-induced scattering of TFG2 cells (Fig. 3D), suggesting that the activation of p42/44 MAPK is involved in both the PE-induced cell cycle arrest and cell scattering. In addition, inhibition of p42/44 MAPK by PD 98059 also markedly blocked PMA-induced cell scattering of TFG2 cells (data not shown).

P38 MAPK has been shown to play important roles in cell proliferation and in morphological changes [8, 15, 17, 42, 43]. Therefore, we tested whether p38 MAPK was also involved in the PE-induced cell cycle arrest and scattering of TFG2 cell. As shown in Fig. 4A, PE rapidly activated p38 MAPK in TFG2 cells, which peaked at 10 min and returned to basal levels within 2 h. PE activation of p38 MAPK was further confirmed by Western blotting analysis using a specific anti-phospho-p38 MAPK antibody (Fig. 4B). Blocking p38 MAPK with 0.5 μM SB203850 or 0.5 μM SB202190 significantly inhibited basal [^{3}H]thymidine uptake. However, these inhibitors did not reverse but rather enhanced the inhibition of the proliferation of TFG2

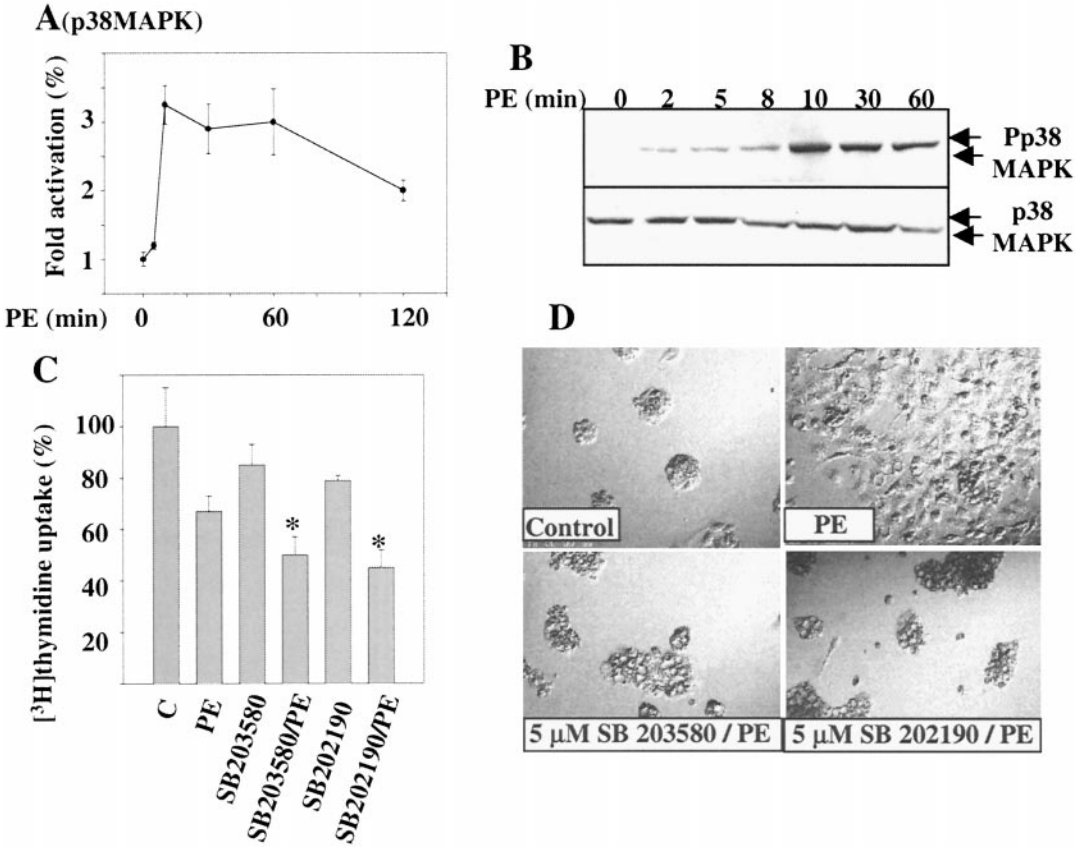

FIG. 4. PE-induced scattering of TFG2 cells is p38 MAPK-dependent. (A) and (B) TFG2 cells were stimulated with PE for various times and then cell lysates were prepared either for p38 MAPK assays by using MBP as a substrate (panel A) or Western blotting analysis by using a specific anti-phospho-p38 MAPK antibody (panel B). The radioactivities on blots from three independent experiments were quantified by phosphorimaging and plotted in panel A. Values shown are means ± SE from three independent experiments, expressed as fold changes over control. (C) TFG2 cells were treated with 0.5 μM SB203580 or SB202190 for 30 min and then stimulated with 10^{-5} M PE for 16 h. [^{3}H]Thymidine (2–5 μCi/ml) was added to the culture for an additional 2 h, and [^{3}H]thymidine incorporation was measured as described under Materials and Methods. Values shown are means ± SE from three independent experiments, expressed as fold changes over control. (D) TFG2 cells were treated with 5 μM SB203580 or SB202190 for 30 min and then stimulated with 10^{-5} M PE for 16 h. The cells were observed under a microscope and the pictures were captured by a video camera.

cells caused by PE (Fig. 4C). The same inhibitors at 5 μM completely prevented the PE-induced scattering of TFG2 cells (Fig. 4D). Five micromolar SB203850 or 5 μM SB202190 almost completely inhibited the PE-induced p38 MAPK activation (data not shown) but did not affect p42/44 MAPK activation (Fig. 3C). These results indicate that the PE-induced scattering of TFG2 cells requires p38 MAPK activation, whereas PE inhibition of TFG2 cell proliferation is independent of p38 MAPK activation. In addition, inhibition of p38 MAPK by SB20190 or SB203850 also markedly blocked PMA-induced cell scattering of TFG2 cells (data not shown).

Activation of PI3 kinase is also known to be involved in ligand-induced changes in cell proliferation and morphology [20, 36, 44–46]. Blocking PI3 kinase activation with two highly specific kinase inhibitors, LY294002 or wortmannin, significantly inhibited basal [^{3}H]thymidine uptake but did not prevent the PE-induced inhibition of cell proliferation and the scattering of TFG2 cells (data not shown). This indicates that the α_1AR-induced cell arrest and scattering are PI3 kinase-independent.

PE-Induced Scattering of TFG2 Cells Is JNK- and c-jun-Dependent

In addition to activation of p42/44 MAPK and p38 MAPK, PE treatment also rapidly activated JNK in TFG2 cells (Fig. 5A), which peaked at 10 to 120 min and returned to basal levels within 4 h. To examine whether activation of JNK is also involved in PE-induced scattering, TFG2 cells were infected with a recombinant adenovirus expressing a dominant-negative JNK, and then stimulated with PE. As shown in Fig. 5E, blocking JNK activation by dominant-negative

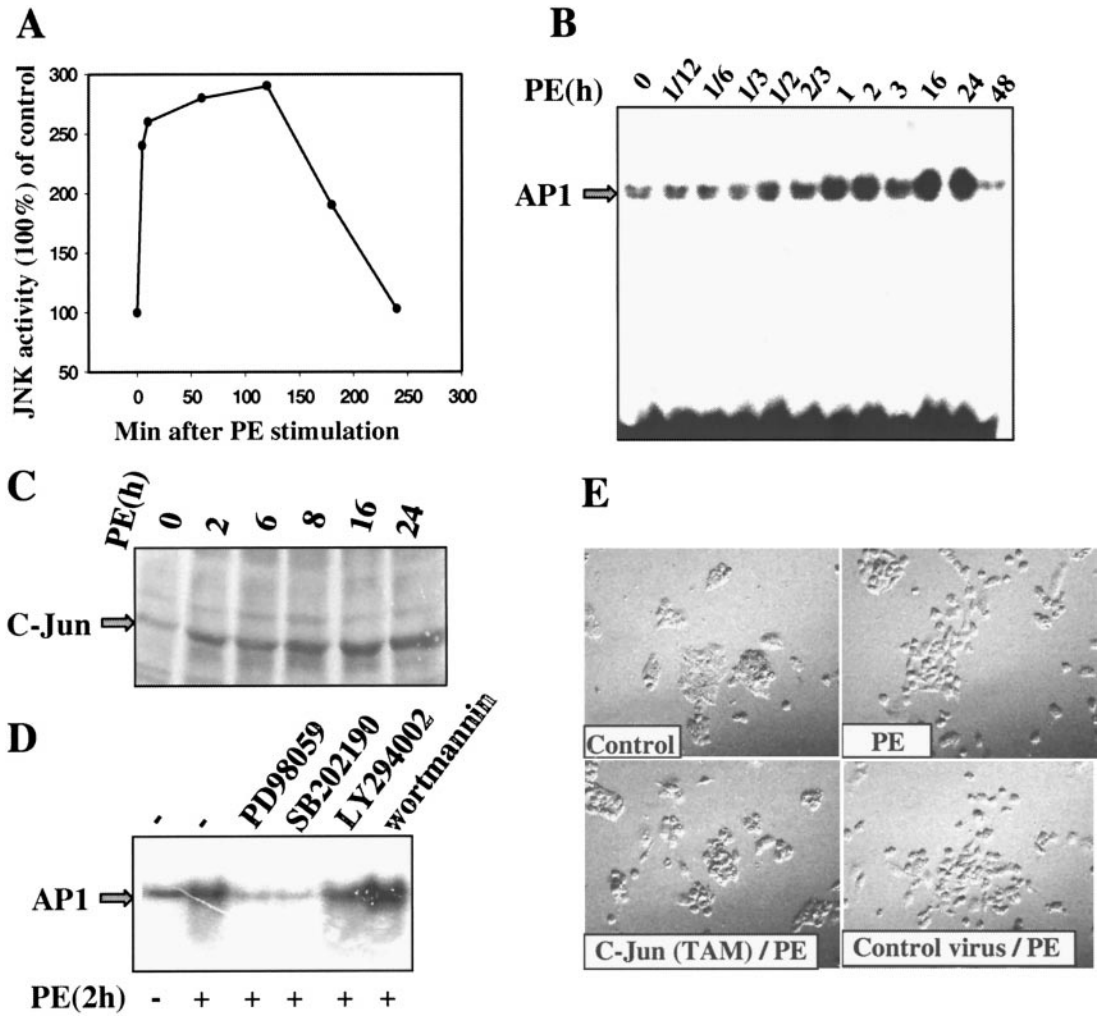

FIG. 5. PE-induced scattering of TFG2 cells is c-jun-dependent. (A–C) TFG2 cells were stimulated with PE for various times and then cell lysates were prepared for JNK assays (A), or DNA gel mobility shift assay by using an AP1 consensus oligonucleotide (B), or Western analysis by using a c-Jun antibody (C). (D) TFG2 cells were treated with 50 μM PD98059, 5 μM SB20219, 20 μM LY294002, or 100 nM wortmannin for 30 min, followed by stimulation with 10^{-5}M PE for 2 h. The protein extracts were then prepared for DNA gel mobility shift assay by using an AP1 oligo. (E) TFG2 cells were infected with a recombinant adenovirus expressing a dominant-negative c-jun (TAM) or a dominant-negative JNK. After 24 h, the cells were stimulated with 10^{-5} M PE for an additional 16 h. The cells were observed under a microscope and the pictures were captured by a video camera.

JNK significantly inhibited PE-induced scattering of TFG2 cells. This suggests that JNK is also involved in PE-induced scattering of TFG2 cells.

P42/44 MAPK, p38 MAPK, and JNK are known to stimulate c-jun gene expression and to phosphorylate the c-Jun protein. To further identify molecular events downstream of MAPK activation, we examined the potential involvement of c-jun in the PE-induced scattering of TFG2 cells. Treatment of TFG2 cells with PE significantly increased AP1 (c-fos/c-jun) binding (Fig. 5B) and c-Jun protein expression (Fig. 5C), and the increase in AP1 binding could be prevented by pretreatment with 50 μM PD98059 or 5 μM SB202190, but not with wortmannin or LY294002 (Fig. 5D). This indicates that PE activates AP1 via p42/44 MAPK and p38 MAPK. Infection of TFG2 cells with a recombinant adenovirus expressing a dominant-negative c-jun (TAM67) significantly inhibited the PE-induced scattering of TFG2 cells, which suggests that c-Jun, a downstream target of p42/44 MAPK, p38 MAPK, and JNK, is also involved in the PE-induced scattering of TFG2 cells. To test whether activation of c-Jun itself is sufficient to scatter HepG2 cells, cells were infected with a recombinant adenovirus expressing the activated v-Jun. After 24 h, the cells were observed under a microscope. Expression of an activated v-Jun caused significant Jun phosphorylation but did not cause cell scattering (data not shown). This suggests that activation of v-Jun itself is not sufficient to scatter HepG2 cells.

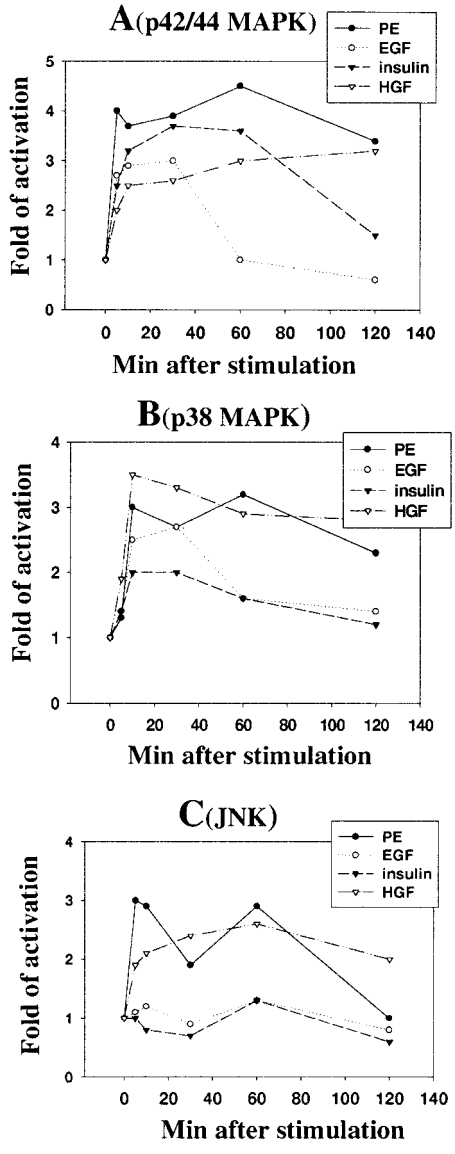

FIG. 6. Activation of p42/44 MAPK, p38 MAPK, and JNK induced by PE, EGF, HGF, and insulin. TFG2 cells were treated with PE (10^{-5} M), EGF (10 ng/ml), HGF (40 ng/ml), or insulin (5 μg/ml) for various periods of time as indicated and then cell lysates were prepared and subjected to p42/44 MAPK (A), p38 MAPK (B), and JNK (C) assays as described under Material and Methods.

Comparisons of Activation of MAPKs by PE, HGF, EGF, and Insulin in TFG2 Cells

The above data showed that PE-induced scattering of TFG2 cells involves all three MAPKs. It is known that HGF, EGF, and insulin also activate MAPKs, yet they do not cause the scattering of TFG2 cells. We therefore compared the effects of PE, HGF, EGF, and insulin on the three MAPKs in TFG2 cells. As shown in Figs. 6A and 6B, PE, HGF, EGF, and insulin treatment significantly activated p42/44 MAPK and p38 MAPK. Activation of p42/44 MAPK and p38 MAPK by PE and HGF is sustained, while activation of these two kinases by EGF and insulin is transient. The data in Fig. 6C show that PE and HGF, but not EGF and insulin, also activate JNK.

DISCUSSION

The present findings represent the first evidence that an agonist of α_1AR is able to induce cell scattering in both transfected HepG2 and M12 cells. It is further demonstrated that the α_1AR-induced scattering of TFG2 cells is PKC-independent, whereas PMA induces scattering via a PKC-dependent mechanism. The failure of PE to cause significant PKC translocation in TFG2 cells (Fig. 2A) may explain the reported inability of a PKC inhibitor to prevent PE-induced activation of ERK1/2 in HEK-293 cells [41]. However, this was an unexpected finding in view of the documented ability of PE to cause cytosol-to-membrane translocation of PKC in rat isolated hepatocytes [47]. This could mean that TFG2 and HEK-293 cells may lack a component required for effective coupling of G-protein coupled receptors to PKC, or that native vs transfected α_1AR have a different ability to couple to PKC.

Evidence is also presented to indicate that activation of p42/44 MAPK and p38 MAPK, but not PI3 kinase, is involved in the α_1AR-induced scattering of TFG2 cells, and that c-Jun, a downstream target of p42/44 MAPK, p38 MAPK, and JNK, is also involved. Taking the present findings and our previously reported observations [29], a model depicting the signaling pathways involved in the PE-induced cell cycle arrest and scattering is presented in Fig. 7. In this model, stimulation of α_{1B}AR leads to activation of p42/44 MAPK, p38 MAPK, JNK, and PI3 kinase. Activation of p42/44 MAPK, p38 MAPK, and JNK, but not PI3 kinase, stimulates the scattering of TFG2 cells. We previously reported that blocking p42/44 MAPK with PD98059 or by a dominant-negative MEK−/− mutant only partially

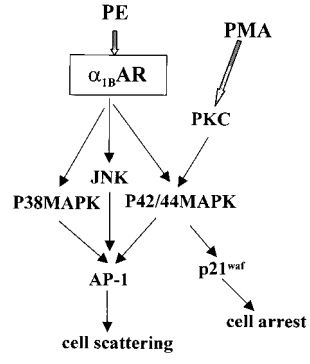

FIG. 7. Model of the signaling pathways involved in α_1AR-mediated cell scattering and cell arrest in TFG2 cells. For explanation, see text.

inhibited the proliferation of TFG2 cells. However, the same treatment abolished PE-mediated inhibition of cell proliferation and unmasked the pro-proliferative effect of PE. This suggests that sustained activation of p42/44 MAPK is involved in PE-induced cell cycle arrest, but not in the ability of PE to promote proliferation [29]. Activation of p42/44 MAPK also triggers the accumulation of the $p21^{waf1/cip1}$ protein, which inhibited the proliferation of TFG2 cells [29], but was found not to be involved in cell scattering. This latter conclusion was based on the finding that transfection of TFG2 cells with a dominant-negative $p21^{waf1/cip1}$ mutant abolished the growth inhibitory effect of PE [29] but did not influence PE-induced cell scattering (Dent *et al.*, unpublished observation). In contrast, activation of AP1 by p42/44 MAPK, p38 MAPK, and JNK activation is involved in the scattering of TFG2 cells. Moreover, two lines of evidence indicate that cell scattering is not due to inhibition of cell proliferation. First, blocking cell proliferation by mitomycin C did not induce cell scattering or increase cell size (data not shown). Second, HGF significantly suppressed HepG2 cell proliferation but did not induce cell scattering (data not shown).

Activation of α_1AR is a powerful pro-proliferative stimulus in different kinds of cells. It triggers the proliferation of hepatocytes [5–8], mycoytes [10–16], and smooth muscle cells [20, 48]. Activation of α_{1A}R also has a hypertrophic effect, as indicated by significant morphological changes in myocytes, including increases in cell size and cell volume and altered sarcomeric organization [3]. Recently, Williams *et al.* [49] reported that the activation of α_{1A}AR, but not α_{2A}AR or βAR, significantly increased the size of transfected PC12 cells. Here we report that an α_1-adrenergic agonist induces cell scattering, cell enlargement, and formation of processes in a malignant hepatoma cell line continuously expressing the α_{1B}AR. These data indicate that activation of α_1AR induces hypertrophy not only in myocardiocytes, but also in other cell types, such as neural cells (PC12 cells [49]), fibroblasts (Rat-1 cells [22]), and hepatic cells (TFG2 cells, present study).

It has been reported that activation of p42/44 MAPK is required for HGF-, PMA-, and EGF-induced scattering of Madin–Darby canine kidney epithelial cells and human stomach adenocarcinoma cells [36, 39]. The activation of p42/44 MAPK is also involved in HGF-induced scattering of HT29 colon carcinoma cells [40]. The present results clearly demonstrate that PE-induced scattering of TFG2 cells requires the activation of p42/44 MAPK, as evidenced by the inhibition of this effect by a highly selective p42/44 MAPK inhibitor, PD98059, or by transfection of a dominant-negative form of MEK1. Unlike p42/44 MAPK [36, 38–40] and PI3 kinase [44–46, 50], which have been implicated in cell scattering induced by HGF, PMA, and EGF, until now there has been no evidence implicating p38 MAPK in cell scattering. In the present study, blocking p38 MAPK activation by two highly selective inhibitors, SB203580 or SB202190, completely prevented the PE-induced scattering of TFG2 cells but did not reverse the PE-induced inhibition of their proliferation, which implicates p38 MAPK in the former, but not in the latter, effect.

The present findings implicate all three MAPKs in the PE-induced spreading of TFG2 cells. Since HGF, EGF, and insulin can also activate the MAPKs, the question arises, why do not these agonists cause spreading of TFG2 cells. The data in Fig. 6 show that PE causes JNK activation and sustained p42/44 MAPK and p38 MAPK activation, while EGF and insulin only elicit transient p42/44 MAPK and p38 MAPK activation. This suggests that JNK activation and sustained p44/42 MAPK and p38 MAPK activation are required for scattering of TFG2 cells. Although HGF causes a similar pattern of activation of all three MAPKs (Fig. 6) and a pattern of inhibition of TFG2 cell proliferation similar to that of PE (unpublished data), it does not induce scattering of HepG2 cells. This suggests that activation of all three MAPKs is necessary but not sufficient for inducing cell scattering, and that some additional signaling pathways are also involved.

The biological significance of PE-induced cell scattering remains unclear. It is well established that cell spreading and migration are crucial for tumor invasion and metastasis. For example, HGF/SF has been shown to be involved in the development of some tumors and in the process of carcinoma cell invasion [51, 52]. If α_1AR-mediated cell scattering occurs *in vivo,* it may promote hepatic tumor cell invasion and metastasis. However, it is interesting to note that a number of malignant hepatoma cell lines and human hepatoma tissue have been found to be devoid of α_{1B}AR or express α_{1B}AR at reduced levels compared to normal liver tissue [27–29]. This suggests that the loss of α_{1B}AR expression by liver tumor cells has complex consequences. On the one hand, it represents the loss of a potential antiproliferative signal [29], which will help tumor growth. On the other hand, the loss of the ability of circulating catecholamines to induce cell scattering could reduce the invasive and metastatic potential of liver tumors. Further studies are aimed to test the effects of stable transfection of α_{1B}AR into hepatoma cells on their *in vivo* tumorigenic, invasive, and metastatic potential. In contrast to liver tumors, α_1ARs are usually present in human prostate cancer [37] and colorectal cancer tissue [53]. The present findings demonstrate that PE treatment can also induce scattering of transfected prostate cancer M12 cells. This suggests that PE-induced cell scattering is not unique to HepG2 cells and activation of α_1AR may induce scattering of prostate cancer cells *in vivo.* If this turns out to be the

case, the routine use of α_1AR antagonists in the treatment of benign prostatic hypertrophy may have the added advantage of inhibiting the invasiveness of potentially coexisting cryptic prostatic tumors.

This work was supported by NIH Grants R29CA72681, R03AA11823, and R01AA12637 (to B.G.). We thank Dr. Michael Birrer (NIH) for providing the v-Jun expression vector and Dr. Joy Ware (Medical College of Virginia) for providing the M12 and p69SV40T prostate cancer cells.

REFERENCES

1. Graham, R. M., Perez, D. M., Hwa, J., and Piascik, M. (1996). Alpha1-adrenergic receptor subtypes: Molecular structure, function, and signaling. *Circ. Res.* **78,** 737–749.
2. Minneman, K. P., and Esbenshade, T. A. (1994). α_1-Adrenergic receptor subtypes. *Annu. Rev. Pharmacol. Toxicol.* **34,** 117–133.
3. Simpson, P. (1985). Stimulation of hypertrophy of cultured neonatal rat heart cells through an α1-adrenergic receptor and induction of beating through an α1- and β1-adrenergic receptor interaction: Evidence for independent regulation of growth and beating. *Circ. Rec.* **56,** 884–894.
4. Knowlton, K. U., Michel, M. C., Itani, M., Shubeita, H. E., Ishihara, K., Brown, J. H., and Chien, K. R. (1993). The alpha 1A-adrenergic receptor subtype mediates biochemical, molecular, and morphologic features of cultured myocardial cell hypertrophy. *J. Biol. Chem.* **268,** 15374–15380.
5. Michalopoulos, G. K. (1990). Liver regeneration: Molecular mechanisms of growth control. *FASEB J.* **4,** 176–187.
6. Cruise, J. L., Knechtle, S. J., Bollinger, R. R., Kuhn, C., and Michalopoulos, G. K. (1987). α1-Adrenergic effects and liver regeneration. *Hepatology* **7,** 1189–1194.
7. Cruise, J. L., Houck, K. A., and Michalopoulos, G. K. (1985). Induction of DNA synthesis in cultured rat hepatocytes through stimulation of α1 adrenergic receptor by norepinephrine. *Science* **227,** 749–751.
8. Spector, M., Auer, K., Jarvis, W., Ishac, E., Gao, B., Kunos, G., and Dent, P. (1997). Differential regulation of MAP and SAP kinase cascade by adrenergic agonists in quiescent and regenerating adult rat hepatocytes. *Mol. Cell. Biol.* **17,** 3556–3565.
9. Auer, K. L., Contessa, J., Brenz-Verca, S., Pirola, L., Rusconi, S., Cooper, G., Abo, A., Wymann, M. P., Davis, R., Birrer, M., and Dent, P. (1998). The Ras/Rac1/Cdc42/SEK/JNK/c-Jun cascade is a key pathway by which agonists stimulate DNA synthesis in primary cultures of rat hepatocytes. *Mol. Biol. Cell.* **9,** 561–573.
10. Thorburn, J., McMahon, M., and Thorburn, A. (1994). Raf-1 kinase activity is necessary and sufficient for gene expression changes but not sufficient for cellular morphology changes associated with cardiac myocyte hypertrophy. *J. Biol. Chem.* **269,** 30580–30586.
11. Bogoyevitch, M. A., Glennon, P. E., and Sugden, P. H. (1993). Endothelin-1, phorbol esters and phenylephrine stimulate MAP kinase activities in ventricular cardiomyocytes. *FEBS Lett.* **317,** 271–275.
12. Bogoyevitch, M. A., Andersson, M. B., Gillespie-Brown, J., Clerk, A., Glennon, P. E., Fuller, S. J., and Sugden, P. H. (1996). Adrenergic receptor stimulation of the mitogen-activated protein kinase cascade and cardiac hypertrophy. *Biochem. J.* **314,** 115–121.
13. Gillespie-Brown, J., Fuller, S. J., Bogoyevitch, M. A., Cowley, S., and Sugden, P. H. (1995). The mitogen-activated protein kinase kinase MEK1 stimulates a pattern of gene expression typical of the hypertrophic phenotype in rat ventricular cardiomyocytes. *J. Biol. Chem.* **270,** 28092–28096.
14. Ramirez, M. T., Sah, V. P., Zhao, X., Hunter, J. J., Chien, K. R., and Brown, J. H. (1997). The MEKK–JNK pathway is stimulated by alpha1-adrenergic receptor and ras activation and is associated with in vitro and in vivo cardiac hypertrophy. *J. Biol. Chem.* **272,** 14057–14061.
15. Zechner, D., Thuerauf, D. J., Hanford, D. S., McDonough, P. M., and Glembotski, C. (1997). A role for the p38 MAP kinase pathway in myocardial cell growth sarcomeric organization, and cardiac-specific gene expression. *J. Cell Biol.* **139,** 115–127.
16. Hoshijima, M., Sah, V. P., Wang, Y., Chien, R., and Brown, J. H. (1998). The low molecular weight GTPase Rho regulates myofibril formation and organization in neonatal rat ventricular myocytes: Involvement of Rho kinase. *J. Biol. Chem.* **273,** 7725–7730.
17. Boluyt, M. O., Zheng, J. S., Younes, A., Long, X., O'Neill, L., Silverman, H., Lakatta, E. G., and Crow, M. T. (1997). Rapamycin inhibits adrenergic receptor-stimulated cardiac myocyte hypertrophy but not activation of hypertrophy-associated genes: Evidence for involvement of p70 S6 kinase. *Circ. Res.* **81,** 176–186.
18. Sah, V. P., Hoshijima, M., Chien, K. R., and Brown, J. H. (1996). Rho is required for Gα_q and α1-adrenergic receptor signaling in cardiomyocytes: Dissociation of Ras and Rho pathways. *J. Biol. Chem.* **271,** 31185–31190.
19. Gottshall, K. R., Hunter, J. J., Tanaka, N., Dalton, N., Becker, K. D., Ross, J., Jr., and Chien, K. R. (1997). Ras-dependent pathways induce obstructive hypertrophy in echo-selected transgenic mice. *Proc. Natl. Acad. Sci. USA* **94,** 4710–4715.
20. Hu, Z. W., Shi, X. Y., Lin, R., and Hoffman, B. B. (1996). α1-Adrenergic receptors activate phosphatidylinositol 3 kinase in human vascular smooth muscle cells: Role in mitogenesis. *J. Biol. Chem.* **271,** 8977–8982.
21. Xin, X., Yang, N., Eckhart, A. D., and Faber, J. E. (1997). Alpha$_{1D}$-adrenergic receptors and mitogen-activated protein kinase mediate increased protein synthesis by arterial smooth muscle. *Mol. Pharmacol.* **51,** 764–775.
22. Allen, L. F., Lefkowitz, R. J., Caron, M. G., and Cotecchia, S. (1991). G-protein-coupled receptor genes as protooncogenes: Constitutively activating mutation of the α1B-adrenergic receptor enhances mitogenesis and tumorigenicity. *Proc. Natl. Acad. Sci. USA* **88,** 11354–11358.
23. Kunos, G., Ishac, E., Gao, B., and Jiang, L. (1995). Inverse regulation of hepatic α_1- and β_2-adrenergic receptors: Cellular mechanisms and physiological implications. *Ann. N. Y. Acad. Sci.* **757,** 261–270.
24. Ishac, E., Lazar-Wesley, E., and Kunos, G. (1992). Rapid inverse changes in hepatic α_1- and β_2-adrenergic receptors and gene transcripts in acutely isolated rat liver cells. *J. Cell. Physiol.* **152,** 79–86.
25. Gao, B., Jiang, L., and Kunos, G. (1996). Transcriptional regulation of α1 adrenergic receptor by nuclear factor 1: A decline in the concentration of nuclear factor 1 correlates with the down-regulation of α_1-adrenergic receptor gene expression in regenerating liver. *Mol. Cell. Biol.* **16,** 5997–6008.
26. Rossby, S. P., and Cornett, L. E. (1991). Steady state levels of hepatic α1 and β2 adrenergic receptors and gene transcripts during development of the male rat. *J. Cell. Physiol.* **147,** 55–61.
27. Bevilacqua, M., Norbiato, G., Chebat, E., Baldi, G., Bertora, P., Regalia, E., Colella, G., Gennari, L., and Vago, T. (1991).

Changes in α1 and β2 adrenergic receptor density in human hepatocellular carcinoma. *Cancer* **67,** 2543–2551.

28. Kost, D. P., DeFrances, M. C., Lee, C. R., and Michalopoulos, G. K. (1992). Patterns of α1 adrenergic receptor expression in regenerating and neoplastic hepatic tissue. *Pathobiology* **60,** 303–308.
29. Auer, K. L., Spector, M. S., Tombes, R. M., Seth, P., Fisher, P. B., Gao, B., Dent, P., and Kunos, G. (1998). α-Adrenergic inhibition of proliferation in HepG2 cells stably transfected with the α_{1B}-adrenergic receptor through a $p42^{MAP\ kinase}/p21^{Cip1/WAF1}$-dependent pathway. *FEBS Lett.* **436,** 131–138.
30. Bae, V. L., Jackson-Cook, C. K., Maygarden, S. J., Plymate, S. R., Chen, J., and Ware, J. L. (1998). Metastatic sublines of an SV40 large T antigen immortalized human prostate epithelial cell line. *Prostate* **34,** 275–282.
31. Kunos, H., Kan, W. H., Greguski, R., and Venter, J. G. (1983). Selective affinity labeling and molecular characterization of hepatic α1 adrenergic receptors with [3H]phenoxybenzamine. *J. Biol. Chem.* **258,** 326–332.
32. Allgood, V. E., Zhang, Y., O'Malley, B. W., and Weigel, N. L. (1997). Analysis of chicken progesterone receptor function and phosphorylation using an adenovirus-mediated procedure for high-efficiency DNA transfer. *Biochemistry* **36,** 224–232.
33. Nyugen, V., and Gao, B. (1999). Cross-talk between α1 adrenergic receptor and interleukin 6 signaling pathways in hepatic cells: Activation of α1 adrenergic receptor inhibits interleukin 6-activated STAT3 by a p42/44 MAP kinase-dependent mechanism. *J. Biol. Chem.* **274,** 35492–35498.
34. Jarvis, W. D., Fornari, F. A., Freemerman, A. J., Szabo, E., Martin, H. A., Rao, A. S., Birrer, M. J., Barbour, S. E., Dent, P., and Grant, S. (1997). Differential requirement for c-Jun in the apoptotic actions of ceramide and sphingosine in human myeloid leukemia cells. *Mol. Pharmacol.* **52,** 935–947.
35. Gao, B., Spector, M. S., and Kunos, G. (1995). The rat α1 adrenergic receptor gene middle promoter contains multiple binding sites for sequence-specific proteins including a novel ubiquitous transcription factor. *J. Biol. Chem.* **270,** 5614–5619.
36. Potempa, S., and Ridley, A. (1998). Activation of both MAP kinase and phosphatidylinositide 3 kinase by Ras is required for hepatocyte growth factor/scatter factor-induced adherens junction disassembly. *Mol. Biol. Cell.* **9,** 2185–2200.
37. Tseng-Crank, J., Kost, T., Goetz, A., Hazum, S., Roberson, K. M., Haizlip, J., Godinot, N., Robertson, C. N., and Saussy, D. (1995). The alpha 1C-adrenoceptor in human prostate: Cloning, functional expression, and localization to specific prostatic cell types. *Br. J. Pharmacol.* **115,** 1475–1485.
38. Zhu, X., and Assoian, R. K. (1995). Integrin-dependent activation of MAP kinase: A link to shape-dependent cell proliferation. *Mol. Biol. Cell.* **6,** 273–282.
39. Tanimura, S., Chatani, Y., Hoshino, R., Sato, M., Watanabe, S., Kataoka, T., Nakamura, T., and Kohno, M. (1998). Activation of the 41/43 kDa mitogen-activated protein kinase signaling pathway is required for hepatocyte growth factor-induced cell scattering. *Oncogene* **17,** 57–65.
40. Herrera, R. (1998). Modulation of hepatocyte growth factor-induced scattering of HT29 colon carcinoma cells: Involvement of the MAPK pathway. *J. Cell. Sci.* **111,** 1039–1049.
41. Della Rocca, G. J., van Biesen, T., Daaka, Y., Luttrell, D. K., Luttrell, L. M., and Lefkowitz, R. J. (1997). Ras-dependent mitogen-activated protein kinase activation by G-protein-coupled receptors: Convergence of G_i- and G_q-mediated pathways on calcium/calmodulin, pyk2 and Src kinase. *J. Biol. Chem.* **272,** 19125–19132.
42. Nemoto, S., Sheng, Z., and Lin, A. (1998). Opposing effects of Jun kinase and p38 MAP kinases on cardiomyocyte hypertrophy. *Mol. Cell. Biol.* **18,** 3518–3526.
43. Wang, Y. B., Huang, S., Sah, V., Ross, J., Brown, J., Han, J., and Chien, K. R. (1998). Cardiac muscle cell hypertrophy and apoptosis induced by distinct members of the p38 MAP kinase family. *J. Biol. Chem.* **273,** 2161–2168.
44. Royal, I., and Park, M. (1995). Hepatocyte growth factor-induced scatter of Madin–Darby canine kidney cells requires phosphatidylinositol 3 kinase. *J. Biol. Chem.* **270,** 27780–27787.
45. Lakkakorpi, P. T., Wesolowski, G., Zimolo, A., Rodan, G. A., and Rodan, S. B. (1997). Phosphatidylinositide 3 kinase association with osteoclast cytoskeleton, and its involvement in osteoclast attachment and spreading. *Exp. Cell Res.* **237,** 296–306.
46. Meng, F., and Lowell, C. A. (1998). A β1 integrin signaling pathway involving Src-family kinases, Cb1 and PI3 kinase are required for macrophage spreading and migration. *EMBO J.* **17,** 4391–4403.
47. Daza, F. J., Parrilla, R., and Martin-Requero, A. (1998). 3,5,3′-Tri-iodo-L-thyronine acutely regulates a protein kinase C-sensitive, Ca^{2+}-independent, branch of the hepatic α1-adrenoreceptor signalling pathway. *Biochem. J.* **331,** 89–97.
48. Chen, L., Xin, X., Eckhart, A. D., Yang, N., and Faber, J. E. (1995). Regulation of vascular smooth muscle growth by alpha 1-adrenoreceptor subtypes in vitro and in situ. *J. Biol. Chem.* **270,** 30980–30988.
49. William, N. G., Zhong, H., and Minneman, K. (1998). Differential coupling of α_1-, α_2-, and β-adrenergic receptors to mitogen-activated protein kinase pathways and differentiation in transfected PC12 cells. *J. Biol. Chem.* **273,** 24624–24632.
50. Khwaja, A., Lehmann, K., Marte, B. M., and Downward, J. (1998). Phosphoinositide 3-kinase induces scattering and tubulogenesis in epithelial cells through a novel pathway. *J. Biol. Chem.* **273,** 18793–18801.
51. Rong, S., Bodescot, M., Blair, D., Dunn, J., Nakamur, T., Mizuno, K., Park, M., Chan, A., Aaronson, S., and Vande Woude, G. F. (1992). Tumorigenicity of the met proto-oncogene and the gene for hepatocyte growth factor. *Mol. Biol. Cell.* **12,** 5152–5158.
52. Bellusci, S., Moens, G., Gaudino, G., Comoglio, P., Nakamura, T., Thierry, J. P., and Jouanneay, J. (1994). Creation of an hepatocyte growth factor/scatter factor autocrine loop in carcinoma cells induces invasive properties associated with increased tumorgenicity. *Oncogene* **9,** 1091–1099.
53. Agrawal, D. K., Wildrick, D. M., and Boman, B. M. (1992). Characteristics of alpha-adrenoceptors in two human colorectal cancer cell lines. *Biochem. Biophys. Res. Commun.* **185,** 176–184.

Received January 31, 2000
Revised version received March 30, 2000